Experimental Eye Research 113 (2013) 172–181

Contents lists available at SciVerse ScienceDirect

Experimental Eye Research

journal homepage: www.elsevier.com/locate/yexer

Specific roles for Group V secretory PLA_2 in retinal iron-induced oxidative stress. Implications for age-related macular degeneration

G. Rodríguez Diez, S. Sánchez Campos, N.M. Giusto, G.A. Salvador*

Instituto de Investigaciones Bioquímicas de Bahía Blanca, Universidad Nacional del Sur and Consejo Nacional de Investigaciones Científicas y Técnicas, 8000 Bahía Blanca, Argentina

ARTICLE INFO

Article history:
Received 8 February 2013
Accepted in revised form 21 May 2013
Available online 18 June 2013

Keywords:
retina
iron
PLA_2
oxidative stress
AMD
acyltransferases

ABSTRACT

Iron accumulation and oxidative stress are hallmarks of retinas from patients with age-related macular degeneration (AMD). We have previously demonstrated that iron-overloaded retinas are a good *in vitro* model for the study of retinal degeneration during iron-induced oxidative stress. In this model we have previously characterized the role of cytosolic phospholipase A_2 ($cPLA_2$) and calcium-independent isoform ($iPLA_2$). The aim of the present study was to analyze the implications of Group V secretory PLA_2 ($sPLA_2$), another member of PLA_2 family, in cyclooxygenase (COX)-2 and nuclear factor kappa B (NF-κB) regulation. We found that $sPLA_2$ is localized in cytosolic fraction in an iron concentration-dependent manner. By immunoprecipitation (IP) assays we also demonstrated an increased association between Group V $sPLA_2$ and COX-2 in retinas exposed to iron overload. However, COX-2 activity in IP assays was observed to decrease in spite of the increased protein levels observed. p65 (RelA) NF-κB levels were increased in nuclear fractions from retinas exposed to iron. In the presence of ATK ($cPLA_2$ inhibitor) and YM 26734 ($sPLA_2$ inhibitor), the nuclear localization of both p65 and p50 NF-κB subunits was restored to control levels in retinas exposed to iron-induced oxidative stress. Membrane repair mechanisms were also analyzed by studying the participation of acyltransferases in phospholipid remodeling during retinal oxidation stress. Acidic phospholipids, such as phosphatidylinositol (PI) and phosphatidylserine (PS), were observed to show an inhibited acylation profile in retinas exposed to iron while phosphatidylethanolamine (PE) showed the opposite. The use of PLA_2 inhibitors demonstrated that PS is actively deacylated during iron-induced oxidative stress. Results from the present study suggest that Group V $sPLA_2$ has multiple intracellular targets during iron-induced retinal degeneration and that the specific role of $sPLA_2$ could be related to inflammatory responses by its participation in NF-κB and COX-2 regulation.

1. Introduction

Iron overload has been found to be associated with retinal degenerative disorders, such as ocular siderosis and the hereditary diseases aceruloplasminemia and human leukocyte antigen-related hemochromatosis (Dunaief et al., 2005; Dunaief, 2006; Hadziahmetovic et al., 2008; Hahn et al., 2004; He et al., 2007; Kell, 2010). In the nervous system and related tissues it has been observed that the increase in iron levels that occur as a result of aging may exacerbate age-related diseases through iron-induced oxidative stress (Hadziahmetovic et al., 2011a). Post *mortem* research has also revealed that iron concentrations and oxidative stress levels are higher in age-related macular degeneration (AMD) retinas than in non-affected retinas (Blasiak et al., 2011; Lukinova

Abbreviations: AA, arachidonic acid; AMD, age-related macular degeneration; AT, acyltransferases; ATK, arachidonoyl trifluoromethyl ketone; Bcl-2, B-cell lymphoma 2; BEL, bromoenol lactone; BSA, bovine serum albumin; CL, cardiolipin; COX, cyclooxygenase; $cPLA_2$, cytosolic phospholipase A_2; Cyt *c*, cytochrome *c*; DTT, dithiothreitol; EDTA, N,N′-1,2-ethandiylbis[N-(carboxymethyl)glycine] disodium salt; GAPDH, glyceraldehyde-3-phosphatedehydrogenase; H&E, haematoxiline and eosine stain; HEPES, 4-(2-hydroxyethyl)-1-piperazine ethanesulfonic acid; hnRNP, heterogeneous nuclear ribonucleoproteins; HRP, horseradish peroxidase; IP, immunoprecipitates; $iPLA_2$, calcium-independent phospholipase A_2; LDH, lactate dehydrogenase; MTT, 3-(4,5-dimethylthiazol-2-yl)-2,5-diphenyltetrazolium bromide; NF-κB, nuclear factor kappa B; PA, phosphatidic acid; PBS, phosphate buffer saline; PC, phosphatidylcholine; PE, phosphatidylethanolamine; PGE_2, prostaglandin E_2; PGF, prostaglandin F; PI, phospatidylinositol; PLA_2, phospholipase A_2; PMSF, phenylmethylsulfonyl fluoride; PS, phosphatidylserine; SDS, sodium dodecyl sulfate; SDS–PAGE, sodium dodecyl sulfate-polyacrylmide gel electrophoresis; SPH, sphingomyelin; $sPLA_2$, secretory phospholipase A_2; TBA, thiobarbituric acid; TBARS, thiobarbituric acid reactive substances; TTBS, Tween-Tris Buffer Saline; YM 26734, $sPLA_2$ inhibitor.

* Corresponding author. Instituto de Investigaciones Bioquímicas de Bahía Blanca, Centro Científico y Tecnológico CONICET Bahía Blanca and Universidad Nacional del Sur, Edificio E1, Camino La Carrindanga km 7, 8000 Bahía Blanca, Argentina. Tel.: +54 291 4861201; fax: +54 291 4861200.
E-mail address: salvador@criba.edu.ar (G.A. Salvador).

0014-4835/$ – see front matter © 2013 Elsevier Ltd. All rights reserved.
http://dx.doi.org/10.1016/j.exer.2013.05.019

et al., 2009). The study of membrane properties, phospholipid metabolism and signaling during iron-induced retinal oxidative stress may therefore contribute to learning about the molecular bases for retinal degenerative diseases.

Remodeling of cellular membranes by phospholipases A_2 (PLA_2) and acyltransferases (AT) is one of the necessary mechanisms for protecting membranes from oxidative damage. Phospholipases A_2 belong to a superfamily composed of a large number of lipolytic enzymes whose common feature is to hydrolyze the fatty acid present in the sn-2 position of glycerophospholipids. At least 30 different PLA_2s or related enzymes have been identified in mammals and have been classified into three main groups: low molecular weight secretory PLA_2 ($sPLA_2$), 85-kDa cytosolic group IV PLA_2 ($cPLA_2$), and calcium-independent group VI PLA_2 ($iPLA_2$) (Chakraborti, 2003). It is now known that these three PLA_2 forms participate in different ways in arachidonic acid (AA) metabolism with their relative contribution being dependent on the cell and the stimulus type. AA release is a highly regulated process that represents the balance between deacylation reaction by PLA_2s and AA reacylation and transfer among different phospholipids by AT and transacylases. AA biological importance lies in its ability to be the precursor of bioactive compounds as is the case of eicosanoids. The latter are produced through oxygenation by two main enzymes, namely cicloxygenases (COX) and lipooxygenases. Due to the potent biological action of these molecules, AA levels must be rigorously controlled and, in resting cells, AA is esterified into phospholipids, as one of the main functions of AT.

$sPLA_2$ represents an important and continuously growing subclass of the PLA_2 superfamily. Similarly to other PLA_2s, it produces free fatty acids and lysophospholipids, both important second messengers in cell signaling, by hydrolyzing the glycerophospholipids present in cell membranes and plasma lipoproteins. $sPLA_2$s can be distinguished from other PLA_2s in terms of their low molecular mass, their high disulfide bond content, and the requirement for millimolar concentrations of Ca^{2+} for catalysis.

It is known that $sPLA_2$ plays an important role in several inflammatory diseases. The first evidence in this respect was from Group IIA $sPLA_2$, which is present at high concentrations in the synovial fluid of patients with rheumatoid arthritis (Seilhamer et al., 1989). Further findings revealed that $sPLA_2$ is a potential amplifier of the amount of AA released by $cPLA_2$ (Kolko et al., 2003; Murakami and Kudo, 2004). Among the different $sPLA_2$s, Group X $sPLA_2$ has been proposed to have an anti-inflammatory activity (Curfs et al., 2008). When $cPLA_2$ is activated, it seems to regulate COX-2 and $sPLA_2$ transcription, which can, in turn, also activate COX-2 transcription (Balboa et al., 2003), thus suggesting the existence of a particular cross-talk between these enzymes.

In a previous work, we characterized the role of $cPLA_2$ and $iPLA_2$ in an *in vitro* model of AMD (Rodríguez Diez et al., 2012) and demonstrated that while $cPLA_2$ promotes the generation of reactive oxygen species, which contribute to oxidative stress in the tissue, $iPLA_2$ plays a protective role against lipid peroxidation. In view of the above, the purpose of the present work was to characterize the role of Group V $sPLA_2$ using iron overload retinas as an *in vitro* AMD model and paying particular attention to different potential molecular targets of Group V $sPLA_2$, such as COX-2, nuclear factor kappa B (NF-κB) and lysophospholipid acyltransferases (AT).

2. Materials and methods

2.1. Materials

[^{14}C]oleoyl-CoA and [^{3}H]arachidonic acid were obtained from New England Nuclear-Dupont (Boston, MA, USA). Triton X-100, 3-(4,5-dimethylthiazol-2-yl)-2,5-diphenyltetrazolium bromide (MTT) and thiobarbituric acid (TBA) were obtained from Sigma–Aldrich (St. Louis, MO, USA). All other chemicals were of the highest purity available. Goat polyclonal anti-group V PLA_2 (T-20), mouse monoclonal anti-heterogeneous nuclear ribonucleoproteins (hnRNP) A1(4B10), rabbit polyclonal anti-NF-κB p65 (A), rabbit polyclonal anti-NF-κB p50 (H-119), rabbit polyclonal anti-cytochrome c (H-104), rabbit polyclonal anti-Bcl-2 (N-19), mouse monoclonal anti-glyceraldehyde-3-phosphatedehydrogenase (GAPDH) (A-3), rabbit polyclonal anti-calnexin (H-70), polyclonal horseradish peroxidase (HRP)-conjugated goat anti-rabbit IgG, polyclonal HRP-conjugated goat anti-mouse IgG, polyclonal HRP-conjugated bovine anti-goat IgG and PLA_2 inhibitors [arachidonoyl trifluoromethyl ketone (ATK), bromoenol lactone (BEL) and YM 26734] were purchased from Santa Cruz Biotechnology, Inc. (Santa Cruz, CA, USA). Rabbit polyclonal anti-COX-2 was purchased from Cayman Chemical (Ann Arbor, MI, USA). Rabbit biotinylated secondary anti-goat antibody was purchased from Vector Laboratories (Burlingame, CA, USA). LDH-P UV AA kit was kindly provided by Wiener lab. Group.

2.2. Experimental treatments

Fresh bovine eyes obtained from a local abattoir were stored in crushed ice. Retinas were dissected on ice (4 °C) under normal lighting conditions and washed with saline solution. In all the experiments retinas were incubated in Locke's buffer [154 mM NaCl, 5.6 mM KCl, 3.6 mM $NaHCO_3$, 1 mM $MgCl_2$, 2.3 mM $CaCl_2$, 5 mM glucose, 5 mM 4-(2-hydroxyethyl)-1-piperazine ethanesulfonic acid (HEPES), pH 7.2] unless stated otherwise under an O_2:CO_2 (95:5, vol/vol) atmosphere with gentle agitation (Rodríguez Diez et al., 2012). After being immersed in Locke's buffer, entire retinas were preincubated for 30 min at 37 °C with either inhibitors (50 μM ATK, 25 μM BEL or 10 μM YM 26734) or vehicle (DMSO) and were subsequently exposed for 60 min to $FeSO_4$ (25, 200 or 800 μM) or its vehicle (ultrapure water) as previously described (Rodríguez Diez et al., 2012). After incubation, retinas were previously washed in saline solution to further proceed with experiments.

2.3. Isolation of subcellular fractions

Homogenates to be used for MTT reduction, thiobarbituric acid reactive substances (TBARS), iron content, Western blot and acyltransferase-activities were prepared in Locke's buffer. Independently of the buffer used, retinas were homogenized by 10 strokes with a Thomas tissue homogenizer [20% (wt/vol), unless indicated otherwise]. Protein content of all retinal subcellular fractions was determined by following Lowry et al. (1951).

For obtaining subcellular fractions, after incubation, homogenates from the dissected retinas were prepared in a medium containing 0.32 M sucrose, 1 mM N,N′-1,2-ethandiylbis[N-(carboxymethyl)glycine] disodium salt (EDTA), 1 mM dithiothreitol (DTT), 2 μg/ml leupeptin, 1 μg/ml aprotinin, 1 μg/ml pepstatin, 0.1 mM phenylmethylsulfonyl fluoride (PMSF), and 10 mM HEPES (pH 7.4). Homogenates were centrifuged at 1800 × *g* for 7.5 min at 4 °C using a JA-21 rotor in a Beckman J2-21 centrifuge. The pellet (corresponding to crude nuclear fraction and cellular debris) was discarded and the supernatant was retained and centrifuged at 14,000 × *g* for 20 min at 4 °C. The mitochondrial pellet was stored at −80 °C and the supernatant was centrifuged at 100,000 × *g* for 1 h at 4 °C using a TLA 100.4 rotor in a Beckman Optima TLX ultracentrifuge. The final pellet was considered as microsomal fraction and the supernatant as cytosolic fraction. Total homogenates, microsomal and cytosolic fractions were used for Western Blot assays.

2.4. Nuclear and cytosolic fraction isolation for the study of NF-κB localization

Nuclear and cytosolic fractions were isolated as previously described (Mackenzie and Oteiza, 2007; Osborn et al., 1999). After treatments, retinas were homogenized using a manual homogenizer (applying 10 strokes) in buffer A [10 mM HEPES, pH 7.9, 1.5 mM $MgCl_2$, 10 mM KCl, 0.5 mM DTT, 0.1% (vol/vol) NP-40, 0.2 M PMSF, 2 μg/ml leupeptin, 1 μg/ml aprotinin, 1 μg/ml pepstatin] in a 200 μl volume of cold buffer to 50 mg of retina. The same volume of buffer A was added and these homogenates were incubated at 4 °C for 10 min and were then centrifuged at 850 × *g* for 15 min. The supernatant (cytosolic fraction) was removed to a pre-chilled microcentrifuge tube and stored at −80 °C until being ready for use, and the nuclear pellet was resuspended in complete buffer lysis, 1 μl/mg of tissue [buffer B: 10 mM HEPES, pH 7.9, 1.5 mM $MgCl_2$, 420 mM NaCl, 0.5 mM DTT, 0.2 mM EDTA, 25% (vol/vol) glycerol, 0.5 mM PMSF, 2 μg/ml leupeptin, 1 μg/ml aprotinin, 1 μg/ml pepstatin]. Samples were incubated for 15 min at 4 °C and centrifuged at 14,000 × *g* for 30 min at 4 °C. The supernatant was transferred to a pre-chilled microcentrifuge tube and stored at −80 °C until used for Western blot analyses.

2.5. Determination of iron content

After incubation in either absence or presence of Fe^{2+}, retinas were washed with saline solution and then homogenized in Locke's buffer for iron analysis. Samples were firstly weighted and their volume was measured. They were subsequently digested with a microwave digestor MARS-5 (CEM Corporation, NC, USA) using 16 M nitric acid (Merck, Bs.As., Argentina), according to SRM 1577a [potency: 400 W; pressure (maximum): 800 psi; temperature (maximum): 200 °C; time: 15 min]. Total cellular iron content was determined by ICP-AES (High Resolution Shimadzu' Simultaneous 9000 according EPA 200.7). Certified reference solutions (QC 21, Spec CentriPrep, Metuchen, NJ, USA) were used to generate the standard curve (Salvador and Oteiza, 2011).

2.6. Morphological analysis and iron detection by Perls' staining

Morphological analysis of tissues was performed using H&E staining. Tissues in non-polarized glass slides were prepared for Perls' staining. Briefly, slides were deparaffinized in xylene for 30 min at 60 °C and rehydrated in a series of ethanol dilutions and water for 5 min in each step. Slides were subsequently incubated in 10% (wt/vol) potassium ferrocyanide for 4 min and were then incubated with working solution [equal parts of 10% (wt/vol) potassium ferrocyanide and 2% (vol/vol) aqueous hydrochloric acid] at room temperature for 10 min, yielding a Prussian blue reaction product. Slides were subsequently washed with distilled water and sensitivity for iron detection was enhanced by incubation in a 0.1% (wt/vol) red nuclear staining solution for 45 s at room temperature, yielding a color contrast reaction. After being dehydrated through graded ethanol and xylene and mounted with Permount (Fisher Scientific), sections were analyzed using a Nikon Eclipse Ti–S microscope (Hadziahmetovic et al., 2011b; Loh et al., 2009).

2.7. MTT reduction assay

To determine mitochondrial retinal reducing capacity, the extent of MTT reduction to insoluble intracellular formazan crystals was measured. This reduction depends on the activity of intracellular dehydrogenases and it is independent of the changes in the integrity of the plasma membrane. MTT reduction was measured in total homogenates obtained from entire retinas exposed to either 25, 200 and 800 μM $FeSO_4$ or vehicle, and in the presence or absence of YM 26734 (Rodríguez Diez et al., 2012).

2.8. Measurement of LDH release

Lactate Dehydrogenase (LDH) release was determined in the incubation medium of the retinas as previously described (Uranga et al., 2007) and using LDH-P UV AA kit, following the manufacturer's instructions. Results were expressed as U/liter.

2.9. Lipid peroxidation assay

Lipid peroxidation was measured using TBA assay as previously described (Rodríguez Diez et al., 2012). TBARS were measured at 535 nm and results were expressed as units of absorbance at 535 nm per mg of protein [Abs 535 nm (arbitrary units)/mg protein].

2.10. Immunoprecipitations and enzyme assays

$sPLA_2$ was immunoprecipitated according to a previously described method (Uranga et al., 2007) with minor modifications. Retinas were homogenized in Triton X-100 lysis buffer [1% (vol/vol) Triton X-100, 137 mM NaCl, 20 mM Tris (pH 8.0), 10% (vol/vol) glycerol, 1 mM ethyleneglycol-bis(beta-aminoethyl ether)-N,N,N′,N′-tetraacetic acid, 1 mM $MgCl_2$, 0.2 mM Na_3VO_4, 1 mM DTT, 2 μg/ml leupeptin, 1 μg/ml aprotinin, 1 μg/ml pepstatin and 0.1 mM PMSF], 2 ml per retina. Insoluble material was removed by centrifugation at 17,000 × *g* for 20 min. Three hundred microliters of solubilized retinal total homogenates were precleared by mixing with 20 μl protein A sepharose (3 mg) for 30 min and briefly spun at 500 × *g*. The supernatant was further incubated overnight with anti-$sPLA_2$ antibody (10 μl) and subsequently mixed with 50 μl protein A sepharose (6 mg) and incubated for 4 h. All incubations were performed with gentle shaking at 4 °C. After a short spin, immunoprecipitates (IPs) were washed three times with PBS. The final IPs were resuspended in 70 μl of COX-2 assay buffer or 30 μl of Laemmli sample buffer (Laemmli, 1970) for COX-2 activity assays and for Western blot analyses. COX-2 activity in IPs was determined by measuring the generation of prostaglandins F and E (PGF_2 and PGE_2) from [^{3}H]arachidonic acid. Enzyme assays were performed in a buffer containing 0.025% (vol/vol) Triton X-100, 0.16 mM $CaCl_2$, 0.2 mg/ml BSA, 4 mM DTT, 100 mM HEPES, pH 7.5 and using $sPLA_2$-IP as enzyme source. The reactions were carried out at 37 °C for 20 min, with gentle agitation, and stopped by the addition of 5 ml of chloroform/methanol (2:1, vol/vol). Prostaglandins were then separated as described by Franchi et al. (2000).

2.11. Acyltransferase activity assays

To determine AT activity, assays were performed as previously described by Castagnet and Giusto (1997), with minor modifications. Briefly, AT activity was determined by measuring the incorporation of [^{14}C]oleate from [^{14}C]oleoyl-CoA into endogenous retinal lysophospholipids. The radioactive substrate was prepared by resuspending [^{14}C]oleoyl-CoA in AT assay buffer and by sonicating this suspension in a sonication bath during 1 min (Castagnet and Giusto, 1997). The assay mixture was incubated in a shaking bath at 37 °C for 20 min. The reaction was stopped by addition of 5.5 ml chloroform/methanol (2:1, vol/vol). Blanks were prepared identically, except that chloroform/methanol was added to the membranes before adding the substrate. Lipids from AT assays were extracted following Folch et al. (1957) and then phospholipids were separated by two dimensional thin layer chromatography according to Mateos et al. (2010). The regions corresponding to phosphatidylcholine (PC), phosphatidylethanolamine (PE),

phosphatidylserine (PS), phospatidylinositol (PI), phosphatidic acid (PA), cardiolipin (CL) and sphingomyelin (SPH) were scraped off and transferred to vials where silica was deactivated by addition of water. Five milliliters of 0.4% (wt/vol) Omnifluor in toluene/Arkopal N-100 (4:1, vol/vol) were subsequently added. Radioactivity in lipid spots from the blanks (typically less than 100 dpm) was subtracted from those of experimental samples. Acyltransferase activity was expressed in dpm per hour per milligram of protein.

2.12. SDS-PAGE and Western blot assays

Samples from total homogenates and microsomal and cytosolic fractions were denatured with Laemmli sample buffer at 100 °C for 5 min (Laemmli, 1970). Equivalent amounts of proteins were separated by SDS-polyacrylamide gel electrophoresis and then transferred to a polyvinylidene fluoride membrane (Millipore, Bedford, MA) using a Mini Trans-Blot cell electroblotter (BIO-RAD Life Science Group, California) for 2 h. Membranes were blocked with 5% (wt/vol) nonfat dry milk in Tween-Tris Buffer Saline (TTBS) [20 mM Tris–HCl, pH 7.5, 100 mM NaCl, and 0.1% (wt/vol) Tween 20] for 1 h at room temperature. Membranes were subsequently incubated with the correspondent primary antibodies [washed three times with TTBS, and then exposed to the appropriate HRP-conjugated secondary antibody (anti-rabbit, anti-mouse or anti-goat) for 1 h at room temperature. Immunoreactive bands were detected by enhanced chemiluminescence (ECL; Amersham Biosciences, USA) using standard X-ray film (ECL, Amersham Biosciences, USA). Immunoreactive bands were quantified using image analysis software (Image J, a freely available application in the public domain for image analysis and processing, developed and maintained by Wayne Rasband at the Research Services Branch, National Institute of Mental Health).

2.13. Statistical analysis

Statistical analysis was performed using one-way ANOVA test to compare means and followed by Fisher's least significant difference (LSD) test. Furthermore, p-values lower than 0.05 were considered statistically significant.

3. Results

3.1. Determination of retinal iron incorporation and cellular damage in iron-induced retinal toxicity

Iron-induced retinal damage characterization was previously evaluated by determining lipid peroxidation levels and cell viability. Thus, entire isolated retinas were incubated in the presence of variable concentrations of $FeSO_4$ (25, 200 and 800 μM) for 60 min. Controls were also assessed, replacing Fe^{2+} by an equal volume of water (vehicle). The generation of malondialdehyde, a marker of lipid peroxidation, was evaluated by measuring TBARS. We previously demonstrated that TBARS generation increased in an Fe^{2+} concentration- and time-dependent manner and that retinal cell viability was affected at 200 and 800 μM Fe^{2+} after 60 min of incubation (Rodríguez Diez et al., 2012). For further characterization of this retinal degeneration model, iron incorporation kinetics was studied. We demonstrated that retinal iron content measured by ICP increased in an Fe^{2+} concentration-dependent manner (Fig. 1A), such increase being 400% at the 200 μM concentration and 1100% at the 800 μM concentration with respect to controls. Iron incorporation was also evaluated by Perls' staining. It was observed that Prussian blue, an indicator of iron presence, was present at 200 μM and significantly increased at 800 μM Fe^{2+}, mainly located in the outer segment layer (Fig. 1B). For further characterizing this *in vitro* model, the expression of cytochrome *c* (Cyt *c*), Bcl-2 and Bax, markers of cell death signaling, was analyzed by Western blot. As shown in Fig. 1C, cytochrome *c* levels were increased in the cytosolic fractions and decreased in the mitochondrial fraction as a function of the $FeSO_4$ concentrations (25, 200 and 800 μM) used. Bcl-2/Bax ratio decreased as a function of iron concentration.

In previous research from our laboratory we described the involvement of $cPLA_2$ in the promotion of lipid peroxidation and

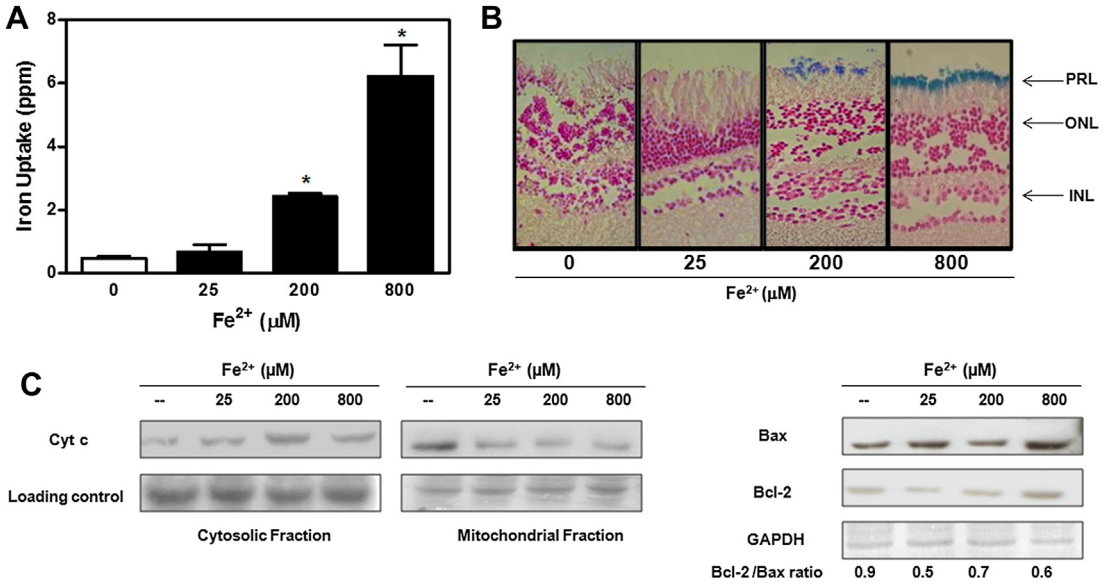

Fig. 1. Determination of iron content and cell death markers in retinas exposed to increasing Fe^{2+} concentrations. (A) Total Fe content was determined in retinal homogenates after exposure to 25, 200, and 800 μM Fe^{2+} for 60 min. Results are shown as ppm and represent the mean ± SD of at least three independent experiments. (B) Retina's Perls Staining performed at the same incubation time and at the same iron concentrations as those described in A. PRL, photoreceptor layer; ONL, outer nuclear layer; INL, inner nuclear layer. (C) Western blot analysis of Cyt *c* in mitochondrial and cytosolic fractions and, Bcl-2 and Bax in cytosolic fractions of retinas incubated under the same experimental conditions as those specified in A. Cyt *c* Bcl-2 and Bax levels were normalized to GADPH levels and represent the mean ± SD of at least three independent experiments. *Significantly different compared to the respective control group ($p < 0.05$, one-way ANOVA test followed by LSD test).

the role of $iPLA_2$ in the protection against lipid peroxidation (Rodríguez Diez et al., 2012). Therefore, to further characterize the role of PLA_2 isoforms, cell viability and lipid peroxidation were analyzed in the presence of YM 26734. Cellular viability and lipid peroxidation levels were observed not to be affected by the presence of YM 26734 (Fig. 2A and B, respectively). For additional characterization of retinal damage, LDH leakage to the incubation medium was measured. Levels of released LDH during iron-induced oxidative stress were compared with those obtained from retinas incubated in a buffer containing 1% Triton-x-100. As shown in Fig. 2C, LDH release under control conditions and in the presence of iron (200 μM) was significantly lower than the levels observed in the presence of a high concentration of detergent, thus indicating that incubation conditions and oxidative stress did not generate important changes in membrane permeability. LDH leakage in the presence and absence of PLA_2 inhibitors, was also determined. Results with ATK, BEL and YM 26734 are shown in Fig. 2D. None of these inhibitors was observed to induce significant changes with respect to control conditions.

3.2. $sPLA_2$ subcellular localization in iron-induced retinal toxicity

Subcellular localization of $sPLA_2$ in retinas exposed to iron-induced oxidative stress was evaluated by Western Blot. A differential iron-induced $sPLA_2$ subcellular localization was observed. This isoform was associated with cytosolic fractions obtained from retinas exposed to iron and the presence of $sPLA_2$ in this fraction increased in an Fe^{2+} concentration-dependent manner (Fig. 3), this increase being 150% at the 200 μM concentration and 90% at the 800 μM Fe^{2+} concentration with respect to controls.

3.3. NF-κB distribution between nuclear and cytosolic fraction during iron-induced retinal toxicity

One of the most common mechanisms triggered by oxidative stress is the activation of the transcription factor NF-κB (Cindrova-Davies et al., 2007; Oeckinghaus et al., 2011). NF-κB p50 is generated by the processing of a larger 105 kDa precursor protein and forms NF-κB complex with NF-κB p65. Under resting conditions both are bound to inhibitory IκB proteins, which sequester NF-κB complexes in the cytoplasm. When stimulus is present, IκB degradation is induced and initiated through phosphorylation by IκB kinase complex (Oeckinghaus et al., 2011). The localization of NF-κB p65 and p50 subunits was affected in response to iron incubation and in the presence of PLA_2 inhibitors. We found that in the presence of iron, both p50 and p65, translocate to the nuclear fraction. In the presence of ATK (50 μM, Fig. 4A) and YM 26734 (10 μM, Fig. 4B), the nuclear localization of both proteins diminished in response to iron-induced oxidative stress. In contrast, BEL (25 μM, Fig. 4A) did not alter NF-κB nuclear localization under oxidative stress conditions. Cytosolic p65 and p50 expression in the presence of iron-induced oxidative stress, however this condition was not affected by the presence of PLA_2 inhibitors (Fig. 4A and B).

3.4. $sPLA_2$ and COX-2 immunoprecipitation in iron-induced retinal toxicity

Recent research from our laboratory has concluded that iron-induced retinal toxicity produces an increase in COX-2 expression and its association with microsomal membranes (Rodríguez Diez et al., 2012). In order to better characterize COX-2 modulation in this iron-induced degeneration model, we studied the association

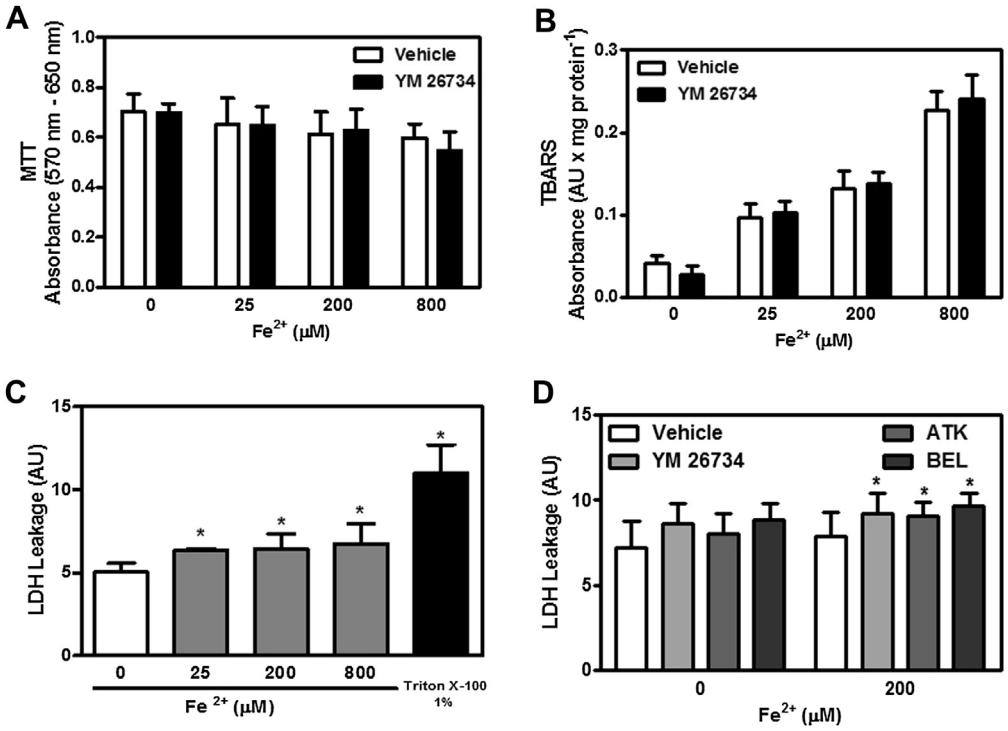

Fig. 2. Characterization of iron-induced retinal damage. (A) Measurement of MTT reduction in homogenates of retinas exposed to 25, 200, and 800 μM Fe^{2+} for 60 min in the presence or absence of $sPLA_2$ inhibitor YM 26734 (10 μM). (B) Lipid peroxidation assay carried out in homogenates of retinas exposed to the same incubation time and the same iron concentrations as those described in A. (C) LDH leakage assay carried out in retinas exposed to increased iron concentrations and in a total lysis condition (1% Triton-X-100). (D) LDH leakage assay performed in retinas exposed to 200 μM Fe^{2+} for 60 min in the presence or absence of ATK (50 μM), BEL (25 μM) and YM 26734 (10 μM). Results are shown as arbitrary units and represent the mean ± SD of at least three independent experiments. *Significantly different compared to the respective control group ($p < 0.05$, one-way ANOVA test followed by LSD test).

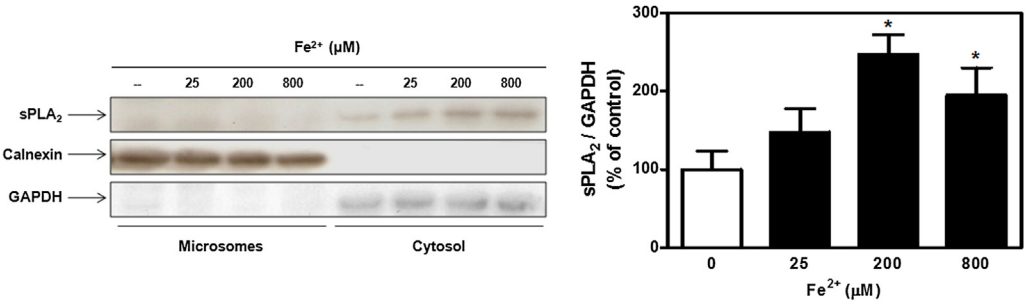

Fig. 3. $sPLA_2$ subcellular localization in retinas exposed to iron-induced oxidative stress. Western blot analysis and quantification of $sPLA_2$ expression in microsomal and cytosolic fractions of retinas (30 μg protein per lane) exposed to 25, 200, and 800 μM Fe^{2+} for 60 min $sPLA_2$ levels in cytosolic fractions were normalized to GADPH levels and expressed as a percentage of the control condition and represent the mean ± SD of at least three independent experiments. *Significantly different compared to the respective control group ($p < 0.05$, one-way ANOVA test followed by LSD test).

between COX-2 and $sPLA_2$. $sPLA_2$ from retinas exposed for 60 min to 200 μM Fe^{2+} was therefore immunoprecipitated to further study if COX-2 co-immunoprecipitates with $sPLA_2$. It could thus be observed that there is an increased association between COX-2 and $sPLA_2$ when retinas are incubated with Fe (Fig. 5A). Prostaglandins generation was also assayed using [^{3}H]arachidonic acid as a substrate in $sPLA_2$ immunoprecipitates. The production of [^{3}H]PGF_2 plus [^{3}H]PGE_2 was diminished in the immunoprecipitates from the retinas exposed to 200 μM Fe^{2+} with respect to controls (Fig. 5B). For additional characterizing the role of $sPLA_2$ on COX-2 modulation, levels of COX-2 expression were evaluated in retinal total homogenates in the presence of YM 26734. The inhibition of $sPLA_2$ activity promoted an increase in COX-2 levels under oxidative stress conditions (Fig. 5C). This increase in COX-2 expression resulted in a major association of COX-2 with $sPLA_2$, as it is shown in immunoprecipitates performed in the presence of YM 26734.

3.5. Acyltransferases activity in iron-induced retinal toxicity

As a counterpart of deacylation mechanisms, phospholipid acylation process in our proposed model was also analyzed. Thus, in order to characterize AT activity in this model, retinas were exposed to Fe^{2+}-induced oxidative stress (200 μM) for 60 min, using [^{14}C] oleoyl-CoA as substrate. The incorporation of [^{14}C]oleic acid was analyzed in PC, PE, PS, PI, PA, CL and SPH (Fig. 6). An increase in PE acylation and a decrease in PS and PI acylation were observed in the retinas incubated in the presence of iron. PC, PA, CL, and SPH showed no changes with respect to controls.

AT activities were also analyzed in the presence of ATK, BEL and YM 26734. PS acylation was observed to be significantly increased and restored to control levels in the presence of ATK in retinas exposed to iron (Fig. 7A). Similar results were obtained for this phospholipid in the presence of BEL and YM 26734 (Fig. 7B and C). Furthermore, a high rate of oleic acid incorporation was observed for PC and PE in the presence of BEL independently of the presence of iron.

4. Discussion

Although the pathogenesis of AMD has not been fully elucidated to date there is a general consensus in support of the participation of oxidative stress and inflammation, both in the onset and

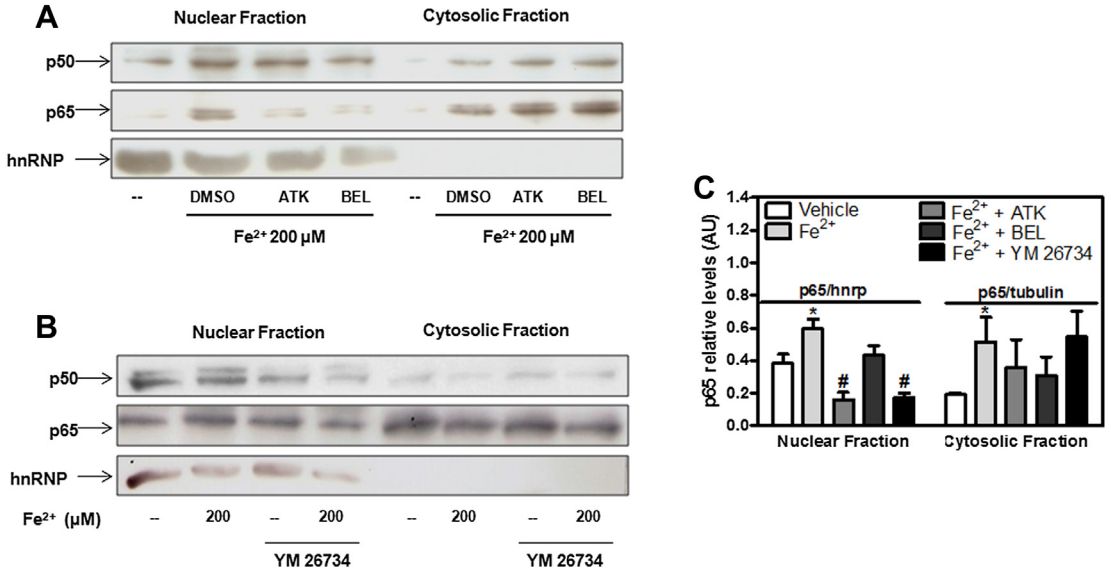

Fig. 4. Involvement of PLA_2 isoforms in NF-κB subcellular localization in retinas exposed to iron-induced oxidative stress. (A) Western blot analysis of NF-κB p65 and p50 subunits in nuclear and cytosolic fractions of retinas (30 μg protein per lane) exposed for 60 min to 200 μM Fe^{2+} in the presence or absence of ATK and BEL (50 μM and 25 μM, respectively). (B) Western blot analysis of p65 and p50 NF-κB subunits in nuclear and cytosolic fractions of retinas (30 μg protein per lane) exposed to the same conditions as those described in A, in the presence or absence of YM 26734 (10 μM). (C) p65 levels were normalized to hnRNP levels in nuclear fractions and to tubulin levels in cytosolic fractions and expressed as arbitrary units. Results represent the mean ± SD of at least three independent experiments. *Significantly different compared to the respective control group ($p < 0.05$, one-way ANOVA test followed by LSD test).

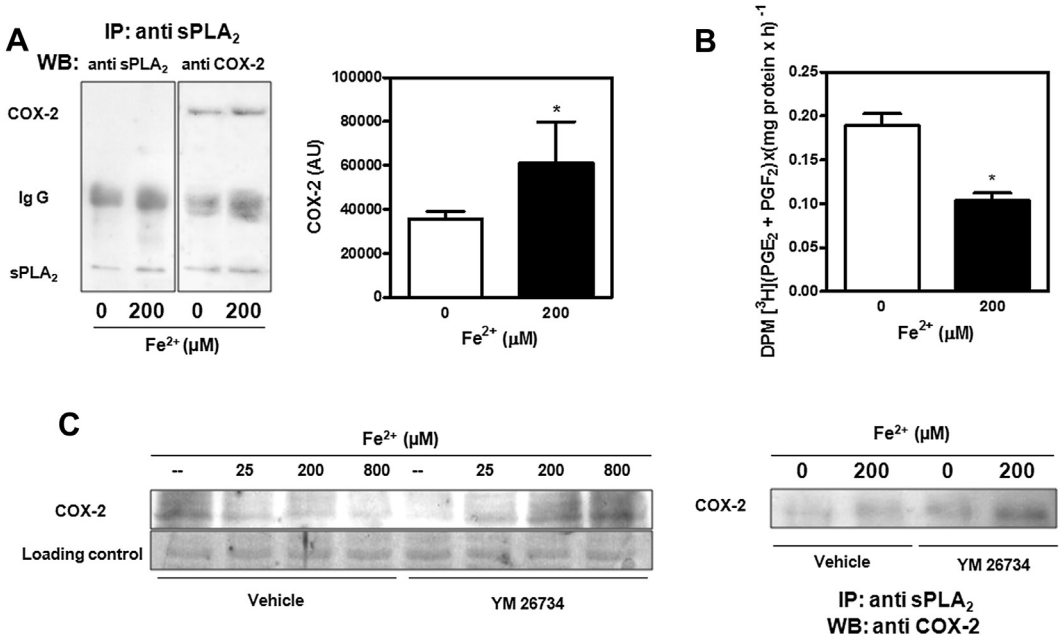

Fig. 5. Association between $sPLA_2$ and COX-2 in retinas exposed to iron-induced oxidative stress. (A) Immunoprecipitation of $sPLA_2$ from retinas exposed for 60 min to 200 μM Fe^{2+}. Immunoprecipitates were resolved in 10% SDS-PAGE gels and analyzed by Western blot and were first incubated with anti-$sPLA_2$ antibody and then with anti-COX-2 antibody. Co-immunoprecipitated COX-2 was quantified and results were expressed as arbitrary units. (B) $sPLA_2$-IPs were also assayed for COX-2 activity using [^{3}H]arachidonic acid as substrate in an appropriate buffer. Reaction products ([^{3}H]PGF_2 and [^{3}H]PGE_2) were extracted, separated by TLC, and quantified by liquid scintillation. Results are expressed as DPM [^{3}H](PGF_2 plus PGE_2) × (mg protein × h)$^{-1}$ and represent the mean ± SD of at least three independent experiments. (C). COX-2 expression levels were determined in retinal total homogenates and in anti-$sPLA_2$ immunoprecipitates in the presence of YM 26734. *Significantly different compared to the respective control group ($p < 0.05$, one-way ANOVA test followed by LSD test).

progression of this devastating disease. Iron accumulation has been reported to be a pathognomonic sign of AMD retinas and has been suspected to be responsible for the high levels of oxidative stress found in these patients (Blasiak et al., 2009, 2011; Dunaief, 2006; Hadziahmetovic et al., 2011a,b; He et al., 2007; Kell, 2010).

It has also been concluded that iron chelation may help in the treatment of several neurological diseases characterized by iron accumulation, such as Alzheimer's disease, Parkinson's disease, Huntington's disease (Youdim et al., 2005) and Friedreich's ataxia (Richardson, 2004; Whitnall et al., 2012). However, it has not yet become an optional treatment for AMD (Dunaief, 2006). For this reason, and in an attempt to better understand the molecular bases of this pathology, the study of the signaling mechanisms triggered during iron-induced retinal degeneration could be helpful for exploring new therapeutic strategies for the treatment of AMD.

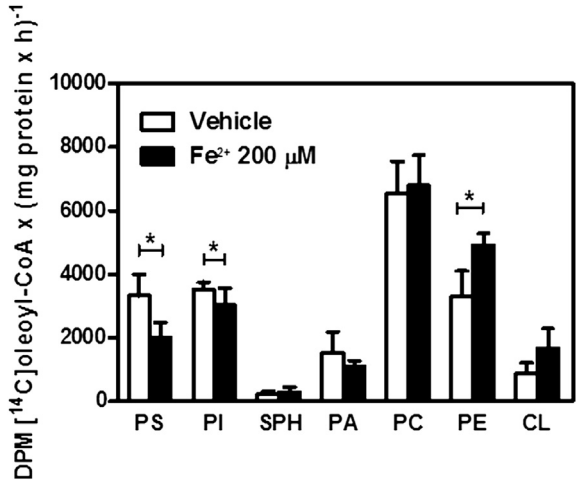

Fig. 6. Acyltransferase activity in retinas exposed to Fe^{2+}-induced oxidative stress. Acyltransferase activity was performed in homogenates of retinas exposed to 200 μM Fe^{2+} for 60 min using [^{14}C]oleoyl-CoA as substrate in an appropriate buffer. Lipids were extracted and phospholipids (PS, PI, SPH, PA, PC, PE and CL) were separated by TLC, and quantified by liquid scintillation. Results are expressed as DPM [^{14}C]oleoyl-CoA × (mg protein × h)$^{-1}$ and represent the mean ± SD of at least three independent experiments. *Significantly different compared to the respective control group ($p < 0.05$, one-way ANOVA test, followed by LSD test).

We have recently characterized an *in vitro* model of AMD and have described the implications of $cPLA_2$ and $iPLA_2$ in retinal damage induced by iron overload (Rodríguez Diez et al., 2012). In the present work, we have further studied the role of $sPLA_2$ in COX-2 and NF-κB regulation and in phospholipid acylation mechanisms during iron-induced retinal injury.

Several isoforms of $sPLA_2$, such as Group IIA and Group X $sPLA_2$, have been traditionally considered to be inflammatory proteins in the peripheral and nervous tissue (Bazan et al., 2002; Moses et al., 2006; Saegusa et al., 2008). In addition, novel anti-inflammatory functions have been recently described for other $sPLA_2$ isoforms, as it is the case of Group V $sPLA_2$ (Boilard et al., 2010). In the present study, we have characterized the role of Group V $sPLA_2$, in particular, during iron-induced retinal damage.

Recent findings from our laboratory showed that while $cPLA_2$ is involved in the generation of retinal damage by promoting lipid peroxidation and COX-2 activation, $iPLA_2$ has a protective role against iron-induced retinal damage (Rodríguez Diez et al., 2012). On the other hand, we show here that retinal functional parameters, such as MTT reduction and membrane permeability, were not found to be affected by the inhibition of $sPLA_2$. Lipid peroxidation levels generated under oxidative stress conditions were observed not to be altered by $sPLA_2$ inhibition. Based on these findings, it could be assumed that $sPLA_2$ does not participate in the mechanisms promoting retinal lipid peroxidation and membrane damage during iron-induced oxidative stress. It was nonetheless observed

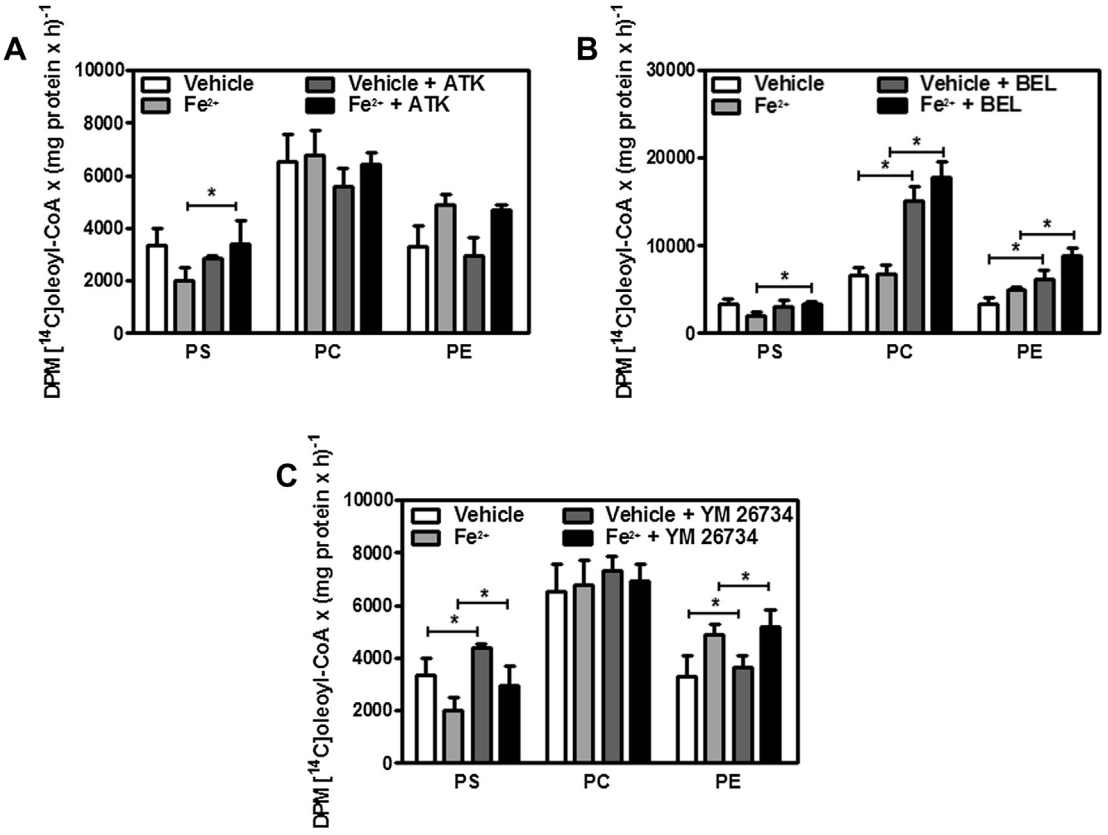

Fig. 7. Relationship between acyltransferase and PLA_2 isoforms activity in retinas exposed to Fe^{2+}-induced oxidative stress. Acyltransferase activity was performed in homogenates of retinas exposed to 200 μM Fe^{2+} for 60 min in the presence or absence of (A) ATK (50 μM), (B) BEL (25 μM) and (C) YM 26734 (10 μM). Lipids were extracted and phospholipids (PS, PI, SPH, PA, PC, PE and CL) were separated by TLC, and quantified by liquid scintillation. Results are expressed as DPM [^{14}C]oleoyl-CoA × (mg protein × h)$^{-1}$ and represent the mean ± SD of at least three independent experiments. *Significantly different compared to the respective control group ($p < 0.05$, one-way ANOVA test, followed by LSD test).

that as iron accumulated, the localization of Group V $sPLA_2$ in the cytosolic fraction increased. This compartmentalization of $sPLA_2$ could be related with its association with COX-2, as shown by IP assays. This association between $sPLA_2$ and COX-2 was also observed in previous studies (Balboa et al., 2003; Ruiperez et al., 2007). In line with this, the increased association of COX-2 with Group V $sPLA_2$ during iron-induced retinal oxidative stress was correlated with a diminished catalytic activity as it was observed by the measuring of PGE_2 and PGF_2 generation on IPs. These results could be indicative of a COX-2 regulatory process exerted by $sPLA_2$ through a mechanism that may involve the sequestration of COX-2 and the inhibition of its catalytic activity. Additionally, the inhibition of $sPLA_2$ activity showed to increase COX-2 expression levels. This increased of $sPLA_2$ expression was coincident with a rise in the association $sPLA_2$-COX-2. Our observations are in agreement with previous findings that propose Group V $sPLA_2$ as an anti-inflammatory agent in an arthritis model, in this particular case by regulating cysteinyl leukotriene synthesis (Boilard et al., 2010).

Since its discovery – more than 25 years ago – as expression regulator of the κ light chain gene in B cells, research on NF-κB keeps on providing novel insights into fundamental cellular processes (Sen, 2011). NF-κB, a key regulator of inflammation, immunity, stress responses, apoptosis and differentiation (Oeckinghaus et al., 2011), has been found to regulate complex gene-expression patterns (Ruland, 2011). It has been demonstrated that dysregulation of NF-κB signaling contributes to the pathophysiology of inflammatory diseases (Oeckinghaus et al., 2011; Smale, 2011). Thus, in our experimental model, the crosstalk between AA release by PLA_2s and NF-κB signaling could be fundamental for understanding the signaling mechanisms that operate during retinal injury triggered by iron-induced oxidative stress. The increased nuclear localization of p50 and p65 NF-κB subunits in the retinas incubated with iron, was abolished by the inhibition of both $cPLA_2$ and $sPLA_2$, thus suggesting that both enzyme activities (that mainly produce AA) are necessary for NF-κB responses during retinal oxidative injury. Accordingly, a direct relationship between $sPLA_2$ and NF-κB activation was reported in foam cells in which LDL hydrolysis by Group V $sPLA_2$ promotes the expression of pro-inflammatory cytokines through the activation of NF-κB transcriptional activity (Boyanovsky et al., 2010).

The involvement of Group V $sPLA_2$ in phospholipid acylation under retinal oxidative stress was also investigated. Quick removal of peroxidized lipids is a mechanism for preserving plasma membrane integrity and cell viability during oxidative stress processes (Murakami et al., 2011). While PLA_2s hydrolyzes free fatty acids in sn-2 position, AT is needed to reacilate this position as well as to maintain normal phospholipid replacement (Perez-Chacon et al., 2009). The increased acylation observed in PE, one of the major membrane phospholipids, and the bare detection of LDH leakage at all iron concentrations assayed, argue in favor of active membrane repair mechanisms during retinal oxidative injury. Furthermore, inhibition in PS and PI acylation during iron-induced retinal toxicity could be related to a high deacylation process probably as a result of the high content of AA present in these phospholipids (Rotstein et al., 1987). In this respect, PS acylation was particularly observed to be increased when $cPLA_2$, $iPLA_2$ and $sPLA_2$ were inhibited, thus demonstrating that during iron-induced oxidative stress conditions this phospholipid is actively deacylated by all PLA_2 isoforms.

Based on findings derived from previous studies and those from our present work, it could be assumed that Group V $sPLA_2$ action

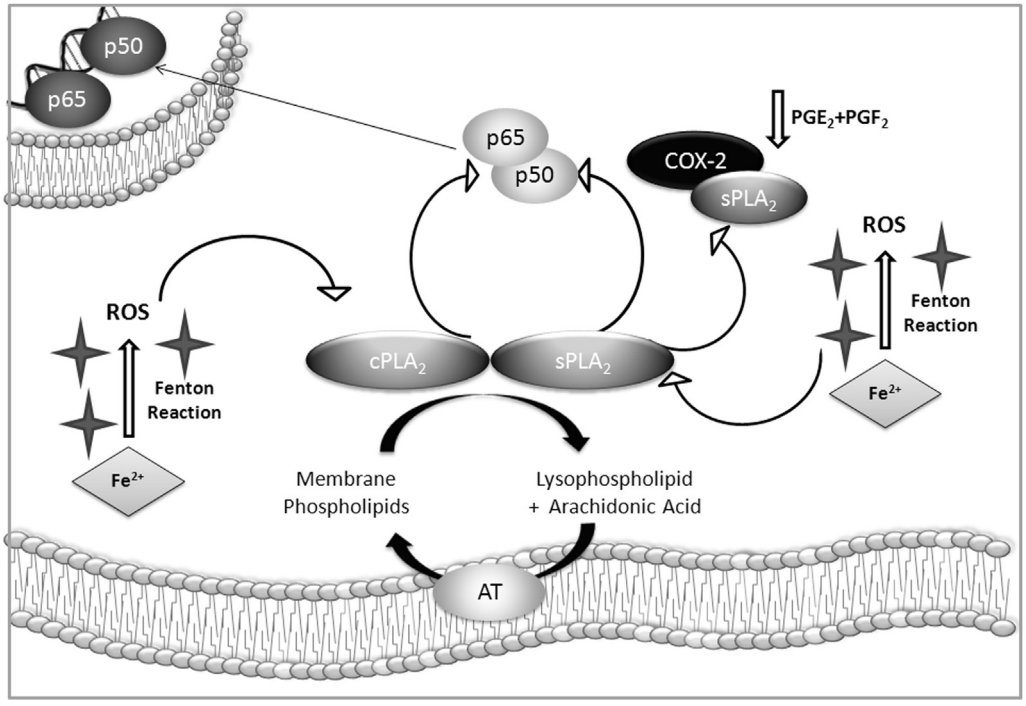

Fig. 8. Schematic view representing signaling pathways involved in retinal response to iron-induced oxidative stress.

during iron-induced retinal toxicity plays a dual role namely as i) an anti-inflammatory agent by inhibiting COX-2 activity, and ii) a pro-inflammatory signal promoting the nuclear localization of NF-κB subunits (Fig. 8). Therefore, deciphering the rules that govern Group V $sPLA_2$-targeted responses during iron-induced retinal degeneration will be a central issue for the search of new therapeutic strategies for treating retinal degeneration induced by oxidative stress.

Funding

This work was supported by grants from the Universidad Nacional del Sur (UNS), the Consejo Nacional de Investigaciones Científicas y Técnicas (CONICET) [grant number PIP 11220090100687], the Fundación Florencio Fiorini and the Agencia Nacional de Promoción Científica y Tecnológica (ANPCYT) [grant number PICT-2010-0936].

Acknowledgments

G.A.S. and N.M.G. are research members of the CONICET. G.R.D. and S.S.C are research fellows of the CONICET. Authors are grateful to Dr. Norberto Ariel Gandini for his technical assistance in the application of histochemical and immunohistochemical techniques and to the staff working at Frigorífico Hilario Viñuelas, particularly to V.M. Daniel Boero, for kindly providing bovine eyes.

Authors specially thank Dr Nicolás Bazán for kindly providing the Group V $sPLA_2$ antibody.

References

Balboa, M.A., Shirai, Y., Gaietta, G., Ellisman, M.H., Balsinde, J., Dennis, E.A., 2003. Localization of Group V phospholipase A2 in caveolin-enriched granules in activated P388D1 macrophage-like cells. J. Biol. Chem. 278, 48059–48065.

Bazan, N.G., Colangelo, V., Lukiw, W.J., 2002. Prostaglandins and other lipid mediators in Alzheimer's disease. Prostaglandins Other Lipid Mediat. 68-69, 197–210.

Blasiak, J., Sklodowska, A., Ulinska, M., Szaflik, J.P., 2009. Iron and age-related macular degeneration. Klin. Oczna. 111, 174–177.

Blasiak, J., Szaflik, J., Szaflik, J.P., 2011. Implications of altered iron homeostasis for age-related macular degeneration. Front. Biosci. 16, 1551–1559.

Boilard, E., Lai, Y., Larabee, K., Balestrieri, B., Ghomashchi, F., Fujioka, D., Gobezie, R., Coblyn, J.S., Weinblatt, M.E., Massarotti, E.M., Thornhill, T.S., Divangahi, M., Remold, H., Lambeau, G., Gelb, M.H., Arm, J.P., Lee, D.M., 2010. A novel anti-inflammatory role for secretory phospholipase A2 in immune complex-mediated arthritis. EMBO Mol. Med. 2, 172–187.

Boyanovsky, B.B., Li, X., Shridas, P., Sunkara, M., Morris, A.J., Webb, N.R., 2010. Bioactive products generated by Group V sPLA(2) hydrolysis of LDL activate macrophages to secrete pro-inflammatory cytokines. Cytokine 50, 50–57.

Castagnet, P.I., Giusto, N.M., 1997. Acyl-CoA: lysophosphatidylcholine acyltransferase activity in bovine retina rod outer segments. Arch. Biochem. Biophys. 340, 124–134.

Chakraborti, S., 2003. Phospholipase A(2) isoforms: a perspective. Cell Signal 15, 637–665.

Cindrova-Davies, T., Spasic-Boskovic, O., Jauniaux, E., Charnock-Jones, D.S., Burton, G.J., 2007. Nuclear factor-kappa B, p38, and stress-activated protein kinase mitogen-activated protein kinase signaling pathways regulate proinflammatory cytokines and apoptosis in human placental explants in response to oxidative stress: effects of antioxidant vitamins. Am. J. Pathol. 170, 1511–1520.

Curfs, D.M., Ghesquiere, S.A., Vergouwe, M.N., van der Made, I., Gijbels, M.J., Greaves, D.R., Verbeek, J.S., Hofker, M.H., de Winther, M.P., 2008. Macrophage secretory phospholipase A2 group X enhances anti-inflammatory responses, promotes lipid accumulation, and contributes to aberrant lung pathology. J. Biol. Chem. 283, 21640–21648.

Dunaief, J.L., 2006. Iron induced oxidative damage as a potential factor in age-related macular degeneration: the Cogan Lecture. Invest. Ophthalmol. Vis. Sci. 47, 4660–4664.

Dunaief, J.L., Richa, C., Franks, E.P., Schultze, R.L., Aleman, T.S., Schenck, J.F., Zimmerman, E.A., Brooks, D.G., 2005. Macular degeneration in a patient with aceruloplasminemia, a disease associated with retinal iron overload. Ophthalmology 112, 1062–1065.

Folch, J., Lees, M., Sloane Stanley, G.H., 1957. A simple method for the isolation and purification of total lipids from animal tissues. J. Biol. Chem. 226, 497–509.

Franchi, A., Di, G.G., Farina, M., de los Santos, A.R., Marti, M.L., Gimeno, M.A., 2000. Differential action of non-steroidal antiinflammatory drugs on human gallbladder cyclooxygenase and lipoxygenase. Medicina (B Aires) 60, 580–586.

Hadziahmetovic, M., Dentchev, T., Song, Y., Haddad, N., He, X., Hahn, P., Pratico, D., Wen, R., Harris, Z.L., Lambris, J.D., Beard, J., Dunaief, J.L., 2008. Ceruloplasmin/hephaestin knockout mice model morphologic and molecular features of AMD. Invest. Ophthalmol. Vis. Sci. 49, 2728–2736.

Hadziahmetovic, M., Song, Y., Ponnuru, P., Iacovelli, J., Hunter, A., Haddad, N., Beard, J., Connor, J.R., Vaulont, S., Dunaief, J.L., 2011a. Age-dependent retinal iron accumulation and degeneration in hepcidin knockout mice. Invest. Ophthalmol. Vis. Sci. 52, 109–118.

Hadziahmetovic, M., Song, Y., Wolkow, N., Iacovelli, J., Kautz, L., Roth, M.P., Dunaief, J.L., 2011b. Bmp6 regulates retinal iron homeostasis and has

altered expression in age-related macular degeneration. Am. J. Pathol. 179, 335–348.
Hahn, P., Qian, Y., Dentchev, T., Chen, L., Beard, J., Harris, Z.L., Dunaief, J.L., 2004. Disruption of ceruloplasmin and hephaestin in mice causes retinal iron overload and retinal degeneration with features of age-related macular degeneration. Proc. Natl. Acad. Sci. U. S. A. 101, 13850–13855.
He, X., Hahn, P., Iacovelli, J., Wong, R., King, C., Bhisitkul, R., Massaro-Giordano, M., Dunaief, J.L., 2007. Iron homeostasis and toxicity in retinal degeneration. Prog. Retin. Eye Res. 26, 649–673.
Kell, D.B., 2010. Towards a unifying, systems biology understanding of large-scale cellular death and destruction caused by poorly liganded iron: Parkinson's, Huntington's, Alzheimer's, prions, bactericides, chemical toxicology and others as examples. Arch. Toxicol. 84, 825–889.
Kolko, M., Rodriguez de Turco, E.B., Diemer, N.H., Bazan, N.G., 2003. Neuronal damage by secretory phospholipase A2: modulation by cytosolic phospholipase A2, platelet-activating factor, and cyclooxygenase-2 in neuronal cells in culture. Neurosci. Lett. 338, 164–168.
Laemmli, U.K., 1970. Cleavage of structural proteins during the assembly of the head of bacteriophage T4. Nature 227, 680–685.
Loh, A., Hadziahmetovic, M., Dunaief, J.L., 2009. Iron homeostasis and eye disease. Biochim. Biophys. Acta 1790, 637–649.
Lowry, O.H., Rosebrough, N.J., Farr, A.L., Randall, R.J., 1951. Protein measurement with the Folin phenol reagent. J. Biol. Chem. 193, 265–275.
Lukinova, N., Iacovelli, J., Dentchev, T., Wolkow, N., Hunter, A., Amado, D., Ying, G.S., Sparrow, J.R., Dunaief, J.L., 2009. Iron chelation protects the retinal pigment epithelial cell line ARPE-19 against cell death triggered by diverse stimuli. Invest. Ophthalmol. Vis. Sci. 50, 1440–1447.
Mackenzie, G.G., Oteiza, P.I., 2007. Zinc and the cytoskeleton in the neuronal modulation of transcription factor NFAT. J. Cell. Physiol. 210, 246–256.
Mateos, M.V., Salvador, G.A., Giusto, N.M., 2010. Selective localization of phosphatidylcholine-derived signaling in detergent-resistant membranes from synaptic endings. Biochim. Biophys. Acta 1798, 624–636.
Moses, G.S., Jensen, M.D., Lue, L.F., Walker, D.G., Sun, A.Y., Simonyi, A., Sun, G.Y., 2006. Secretory PLA2-IIA: a new inflammatory factor for Alzheimer's disease. J. Neuroinflammation 3, 28.
Murakami, M., Kudo, I., 2004. Secretory phospholipase A2. Biol. Pharm. Bull. 27, 1158–1164.
Murakami, M., Taketomi, Y., Sato, H., Yamamoto, K., 2011. Secreted phospholipase A2 revisited. J. Biochem. 150, 233–255.
Oeckinghaus, A., Hayden, M.S., Ghosh, S., 2011. Crosstalk in NF-kappaB signaling pathways. Nat. Immunol. 12, 695–708.
Osborn, M.T., Herrin, K., Buzen, F.G., Hurlburt, B.K., Chambers, T.C., 1999. Electrophoretic mobility shift assay coupled with immunoblotting for the identification of DNA-binding proteins. Biotechniques 27, 887–890, 892.
Perez-Chacon, G., Astudillo, A.M., Balgoma, D., Balboa, M.A., Balsinde, J., 2009. Control of free arachidonic acid levels by phospholipases A2 and lysophospholipid acyltransferases. Biochim. Biophys. Acta 1791, 1103–1113.
Richardson, D.R., 2004. Novel chelators for central nervous system disorders that involve alterations in the metabolism of iron and other metal ions. Ann. N. Y. Acad. Sci. 1012, 326–341.
Rodríguez Diez, G., Uranga, R.M., Mateos, M.V., Giusto, N.M., Salvador, G.A., 2012. Differential participation of phospholipase A(2) isoforms during iron-induced retinal toxicity. Implications for age-related macular degeneration. Neurochem. Int. 61, 749–758.
Rotstein, N.P., Ilincheta de Boschero, M.G., Giusto, N.M., Aveldano, M.I., 1987. Effects of aging on the composition and metabolism of docosahexaenoate-containing lipids of retina. Lipids 22, 253–260.
Ruiperez, V., Casas, J., Balboa, M.A., Balsinde, J., 2007. Group V phospholipase A2-derived lysophosphatidylcholine mediates cyclooxygenase-2 induction in lipopolysaccharide-stimulated macrophages. J. Immunol. 179, 631–638.
Ruland, J., 2011. Return to homeostasis: downregulation of NF-kappaB responses. Nat. Immunol. 12, 709–714.
Saegusa, J., Akakura, N., Wu, C.Y., Hoogland, C., Ma, Z., Lam, K.S., Liu, F.T., Takada, Y.K., Takada, Y., 2008. Pro-inflammatory secretory phospholipase A2 type IIA binds to integrins alphavbeta3 and alpha4beta1 and induces proliferation of monocytic cells in an integrin-dependent manner. J. Biol. Chem. 283, 26107–26115.
Salvador, G.A., Oteiza, P.I., 2011. Iron overload triggers redox-sensitive signals in human IMR-32 neuroblastoma cells. Neurotoxicology 32, 75–82.
Seilhamer, J.J., Pruzanski, W., Vadas, P., Plant, S., Miller, J.A., Kloss, J., Johnson, L.K., 1989. Cloning and recombinant expression of phospholipase A2 present in rheumatoid arthritic synovial fluid. J. Biol. Chem. 264, 5335–5338.
Sen, R., 2011. The origins of NF-kappaB. Nat. Immunol. 12, 686–688.
Smale, S.T., 2011. Hierarchies of NF-kappaB target-gene regulation. Nat. Immunol. 12, 689–694.
Uranga, R.M., Mateos, M.V., Giusto, N.M., Salvador, G.A., 2007. Activation of phosphoinositide-3 kinase/Akt pathway by $FeSO_4$ in rat cerebral cortex synaptic endings. J. Neurosci. Res. 85, 2924–2932.
Whitnall, M., Suryo, R.Y., Huang, M.L., Saletta, F., Lok, H.C., Gutierrez, L., Lazaro, F.J., Fleming, A.J., St Pierre, T.G., Mikhael, M.R., Ponka, P., Richardson, D.R., 2012. Identification of nonferritin mitochondrial iron deposits in a mouse model of Friedreich ataxia. Proc. Natl. Acad. Sci. U. S. A. 109, 20590–20595.
Youdim, M.B., Fridkin, M., Zheng, H., 2005. Bifunctional drug derivatives of MAO-B inhibitor rasagiline and iron chelator VK-28 as a more effective approach to treatment of brain ageing and ageing neurodegenerative diseases. Mech. Ageing Dev. 126, 317–326.